A new age-dating model for cool main sequence stars that combines stellar evolution models with gyrochronology

ABSTRACT

By combining two different sets of observable stellar properties and dating methods that are sensitive to two different evolving processes in stars, core hydrogen burning and magnetic braking, it is possible to infer more precise and accurate ages than using either method in isolation. In this investigation, the observables of main sequence stars that are used to trace core hydrogen burning and stellar evolution on the Hertzprung-Russell diagram ($T_{\rm eff}$, [Fe/H], log g, parallax, apparent magnitude and photometric colors) are combined with their *Kepler* rotation periods, in a Bayesian framework, to infer stellar ages from both stellar evolution models/isochrone placement and gyrochronology. We show that incorporating rotation periods into stellar evolution models significantly improves the precision of inferred ages on the main sequence. However, since ages predicted with gyrochronology are, in general, much more precise than isochronal ages but not necessarily more accurate, care must be taken to ensure either a) the gyrochronology relation being used *is* accurate, or b) its precision is relaxed by introducing a mixture model or some intrinsic scatter or similar. In this pilot study we do not aim to produce a new state-of-the-art dating model, or an improved gyrochronology model, our goal is simply to explore the process of combining two independent dating methods. Although calibration is not the main purpose of this exploratory investigation and the parameters of our gyrochronology model are fixed, only a slight modification to our algorithm would be required to perform a calibration. Accompanying this publication is open source, packaged and documented code, for measuring stellar ages from spectroscopic parameters and/or apparent magnitudes, parallaxes and rotation periods.

1. Introduction

The formation and evolution of the Milky Way (MW) and the planetary systems within it are two topics of significant interest in astronomy today. Both of these fields require precise and accurate ages of tens to hundreds of thousands of stars. Precise ages of red giant

stars, some calculated from asteroseismology, some from spectroscopy, some from physical models and some from machine learning methods have recently been used to explore the age distributions of stellar populations in the MW (*e.g.* Ness et al. 2015; Stello et al. 2017; Das and Sanders 2018; Sanders and Das 2018). Red giants are highly luminous and can be observed to great distances, thus providing age information on the scale of tens of kilo-parsecs. Main sequence (MS) stars on the other hand, although fainter, are more numerous and so their ages may provide new insights into the formation and evolution of the Solar neighborhood. MS star ages are also of great interest for studying the formation and evolution of planetary systems. Almost all exoplanets discovered to date orbit MS stars and it is therefore *MS star* ages that are needed to study planet evolution. Unfortunately, the very property that makes MS stars good hosts for habitable planets also makes them difficult to date: they do not change substantially over time.

The difficulty of age-dating is particularly acute for low mass (GKM) stars on the MS: precisely those that comprise the majority of known planet hosts. Using conventional dating methods, uncertainties on the ages of these stars can be as large as the age of the Universe, *i.e.* they are completely unconstrained. The stars eligible for *truly* precise age-dating, where age uncertainties can be as low as 10%, are those in nearby open clusters, those with observable acoustic oscillations (asteroseismic stars), those just turning off the MS, and the Sun (see **?**, for a review of stellar ages). There are only a few tens of cool, MS stars with precise ages that are suitable for exoplanet population studies, however *tens-of-thousands* of precise ages are needed to study the evolution of planetary systems. The number of planets detected in open clusters, therefore with precise ages, is growing, however there are still only a couple of dozen of these discovered so far and the total number of detectable planets in clusters is unlikely to reach statistical numbers in the near future, if ever. In order to study the evolution of planetary systems, a significant number of precise ages for cool MS *field* stars are needed. Neither cluster stars nor asteroseismic stars can currently provide the numbers required for exoplanet population studies: age-dating methods for cool MS field stars *must* be improved before the evolution of planets can be explored.

The spectra and colors of MS stars do not contain a significant amount of age information because they do not change rapidly. This is represented in the spacing of isochrones on a Hertsprung-Russell (HR) or color-magnitude diagram (CMD). On the MS, isochrones are tightly spaced and, even with very precise measurements of effective temperature and luminosity, the position of a MS star on the HR diagram may be consistent with range of isochrones spanning several billion years. At main sequence turn-off however, isochrones are spread further apart, so that sufficiently precisely measured temperatures and luminosities may yield ages that are extremely precise. The classical method for measuring stellar ages is isochrone placement, or isochrone fitting, where surface gravity changes resulting from

fusion in the core (usually observed via luminosity, L, and effective temperature, $T_{\rm eff}$, or absolute magnitude and colour) are compared with a set of models that trace stellar evolution across the Hertzprung-Russell, or color-magnitude diagram (CMD). Surface gravity changes have been thoroughly mapped with physical models, and can be used to calculate relatively accurate (but not necessarily precise) ages, barring some small, $\sim$10% variations between different models. Isochronal ages *can* be precise for stars turning off the MS, because the rate of change in brightness and temperature is large during this phase of stellar evolution. However, on the MS itself, there is little differentiation between stars of different ages in the L and $T_{\rm eff}$ plane, so ages tend to be very imprecise. Gyrochronology, the method of inferring a star's age from its rotation period is much better suited to measuring ages on the MS.

The gyrochronology model used to calculate the Fisher information is a simple polynomial model, fit to Praesepe and the Sun only. The minimum theoretical absolute age uncertainty (left panel) ranges from tens of millions to a few billion years (up to around 3 Gyr for old G dwarfs). This is the minimum theoretical precision given the adopted gyrochronology model and, since the model used for this calculation does not include intrinsic scatter which is particularly large for young stars, the minimum age uncertainty for young stars is over-optimistic. Similarly, our model does not account for weakened magnetic braking at old ages (van Saders et al. 2016) so is also optimistic for old dwarfs.

Asteroseismology can provide precise ages of *both* red giant and MS stars but due to the greater quantity of observations suitable for *red giant* asteroseismology, precise red giant asteroseismic ages outnumber MS ages. The typical periods of red giant acoustic pulsations are long (on the orders of hours to weeks) and can be detected using *Kepler*'s long cadence mode of one observation per thirty minutes, *Kepler*'s standard and most common observing mode. In addition, the amplitudes of red giant pulsations are typically very large, significantly greater than *Kepler*'s photometric noise floor. MS stars, on the other hand, oscillate with periods of just a few minutes and the long cadence *Kepler* observations, taken once every half-hour, are far above the Nyquist limit and not capable of resolving these pulsations. Asteroseismic measurements of MS stars can only be made when observed in *Kepler*'s short cadence mode of one observation every minute. However, since the amplitude of pulsation scales with stellar radius, the majority of stars with asteroseismic ages successfully measured using *Kepler* short-cadence observations, of which there are currently around 500 (Chaplin et al. 2014), are subgiants. Only $\sim$30 of these are truly on the MS. This may change soon however: *Kepler*'s short cadence light curves have recently been reprocessed and new, precise ages for the *all* stars observed in short cadence mode (around 2000 in the original *Kepler* mission) may be measured and made available soon.

The Sun's rotation period will vary by almost an order of magnitude over its MS lifetime

Fig. 1.— This figure shows Solar-metallicity MIST isochrones in *Gaia* absolute G-band magnitude and Gaia $G_{BP} - G_{RP}$ color. In the left panel the isochrones are colored by the minimum absolute age uncertainty at each point on the CMD, calculated using the Fisher information, based on the typical uncertainties of *Gaia* photometry (represented by black errorbars in the upper right). The purple color in the top left corresponds to small age uncertainties, *i.e.* good age precision. Age precision increases as stars begin to turn off the MS. On the MS however, particularly at low masses, the age precision is poor. For late K dwarfs, for example, isochrone fitting age uncertainties exceed the age of the Universe. This makes sense when you consider that typical *Gaia* uncertaintes on G and $G_{BP} - G_{RP}$ exceed the entire width of the MS, which spans 0.01-14 Gyrs. Isochrone fitting is not an appropriate age-dating method for MS stars, especially at low masses. In the right panel the isochrones are colored by the logarithmic *relative* age precision at each point in the CMD. Relative age uncertainties range from 100% for the oldest MS GKM stars, to several thousand percent for the youngest. These age uncertainties were calculated using the derivatives of G and $G_{BP} - G_{RP}$ with age, *i.e.* the rate of change in a star's luminosity and temperature. For example, K dwarf temperatures increase at a rate of only around 20 K per billion years. The precision with which an age can be measured is related to the separation between isochrones, which indicate epochs of rapid change (steep gradients).
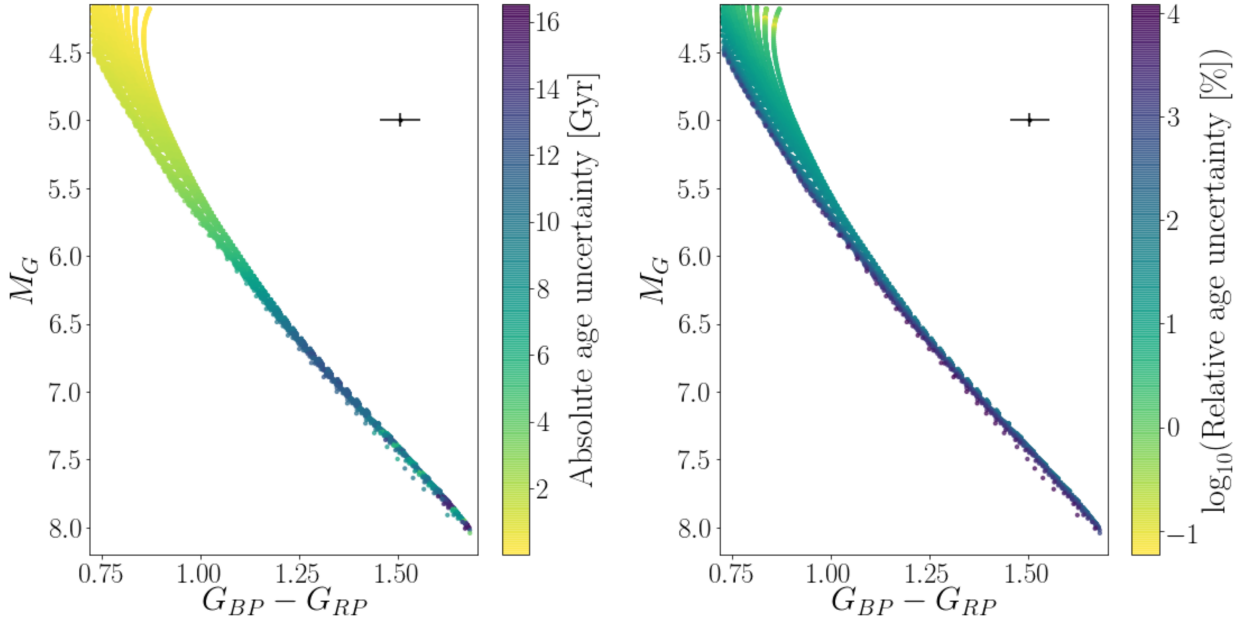
Fig. 2.— As figure 1, however in this case the minimum age uncertainties are calculated based on isochrone fitting and gyrochronology *combined*. The isochrones are colored by the minimum relative age uncertainty at each point on the CMD, based on the typical uncertainties of Gaia photometry and Kepler rotation period uncertainties (assumed to be around 1 day). In contrast to figure 1, here the left panel shows the *logarithmic* absolute age and the right panel shows the linear relative age. The isochrones still supply precise ages at the MS turn off (purple, upper left) however, gyrochronology supplies precise ages on the MS (15 - 25% relative precision). Gyrochronology and isochrone fitting complement each other and when used together, all subgiants and MS stars can have ages more precise than 30%.
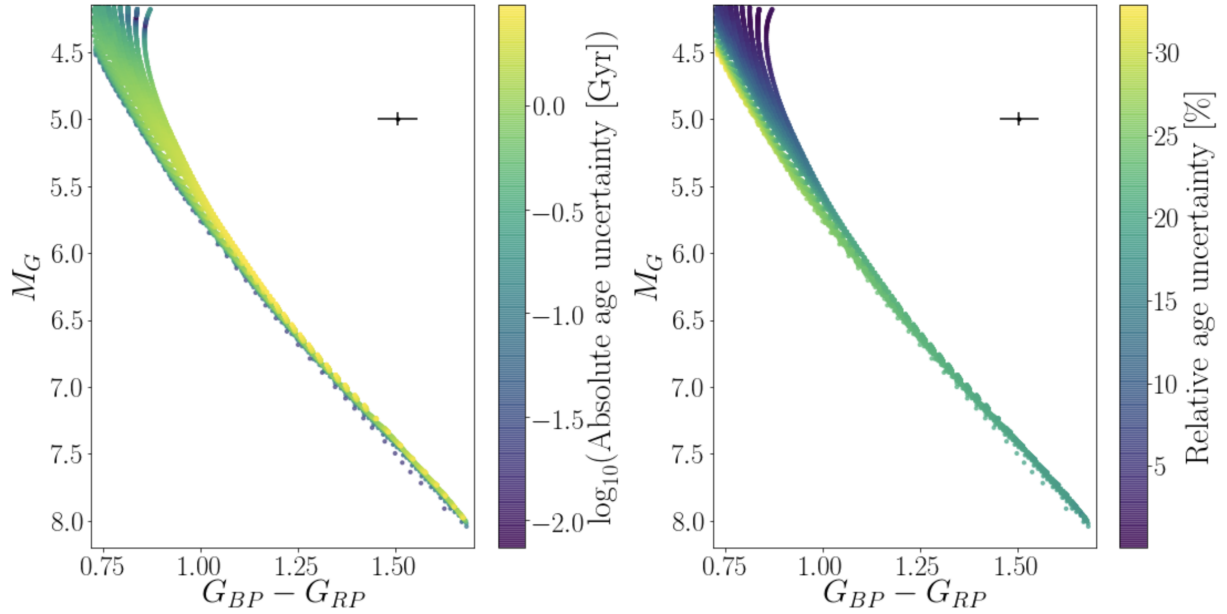
due to magnetic braking. In contrast, luminosity and temperature are not sensitive age proxies for Sun-like stars, are often inferred indirectly, and can be difficult to infer precisely. In addition, the precision with which the luminosity and temperature of a star can be measured is highly sensitive to its distance and the amount of extincting dust along the line of sight. Stellar rotation periods are much more sensitive to age than luminosity or temperature and can be measured precisely, with little dependence on distance and none on extinction, directly from *Kepler* light curves. Gyrochronology, the dating method that uses stellar rotation periods, has the potential to provide MS star ages that are precise to around 20% (Epstein and Pinsonneault 2014). Due to the abundance of rotation periods of MS stars already provided by *Kepler/K2* and the many more expected from future photometric surveys, gyrochronology is one of the most readily available methods for inferring precise stellar ages and, as such, has gained interest over the last few years.

Magnetic braking in MS stars was first observed by Skumanich (1972) who, studying young clusters and the Sun, found that the rotation periods of Solar-type stars decay with the square-root of time. It has since been established that the rotation period of a star depends, to first order, only on its age and mass (*e.g.* Barnes 2003). This means that by measuring a star's rotation period and a suitable mass proxy (B-V color is commonly used), one can determine its age. The convenient characteristic of stars that allows their ages to be inferred from their *current* rotation periods and independently of their primordial ones, comes from the steep dependence of spin-down rate on rotation period (Kawaler 1989). This means that a star spinning with high angular velocity will experience a much greater angular momentum loss rate than a slowly spinning star. For this reason, no matter the initial rotation period of a Sun-like star, after around 500 million years stellar rotation periods appear to converge onto a tight sequence citation. After this time, the age of a star can be inferred, to first order, from its mass and rotation period alone; this is the principle behind gyrochronology.

The relation between age, rotation period and mass has been studied in detail, and several different models have been developed to capture the rotational evolution of Sun-like stars. Some of these models are theoretical and based on physical processes; modeling angular momentum loss as a function of the stellar properties as well as the properties of the magnetic field and stellar wind (Kawaler 1988, 1989; van Saders and Pinsonneault 2013; Matt et al. 2015; van Saders et al. 2016). Other models are empirical and capture the behavior of stars from a purely observational standpoint, using simple functional forms that can reproduce the data (Barnes 2003, 2007; Mamajek and Hillenbrand 2008; Angus et al. 2015). Both types of model, theoretical and empirical, must be calibrated using observations. Old calibrators are especially important because new evidence suggests that rotational evolution goes through a transition at old age or, more specifically, at a large Rossby number, *Ro* (the ratio of rotation period to the convective overturn timescale). For example, old *Kepler* asteroseismic

stars rotate more rapidly than expected given their age (*e.g.* Angus et al. 2015; van Saders et al. 2016). A new physically motivated gyrochronology model, capable of reproducing these data, was recently introduced (van Saders et al. 2016). It relaxes magnetic breaking at a critical Rossby number of around the Solar value, 2.1. This model predicts that, after stellar rotation periods lengthen enough to move stars cross this Ro threshold, stars stop spinning down and maintain a constant rotation period from then until they evolve off the MS. The implication is that the ages of stars with $Ro > 2.1$ cannot be measured from their rotation periods. Despite recent advances in rotation-dating, such as the new Ro transition models (van Saders et al. 2016, 2018), there is still substantial room for improvement in the gyrochronology relations.

The gyrochronology models that capture post Ro-threshold, rotational evolution (van Saders et al. 2016) are the current state-of-the-art in rotation dating. These models are expensive to compute and, just as with most isochrones and stellar evolution tracks, are usually pre-computed over a grid of stellar parameters, then interpolation is used to predict the age of a star. The process of measuring a stellar age with these models is similar to inferring an age using any set of isochrones, with the main difference being that rotation period is an additional dimension. Ages calculated using these models are therefore likely to be much more precise than using rotation-free isochrones since rotation period provides an additional anchor-point for the age of a star. We present here a complementary method that combines isochrones with an *empirical* gyrochronology model using a Bayesian framework. The methodology is related to the models described above (van Saders et al. 2016) in that both use a combination of rotation periods and other observable properties that track stellar evolution on the HR diagram in concert. The main difference is that the gyrochronology model used here is an entirely empirically calibrated one, as opposed to a physically derived one. One major advantage of using a physically motivated gyrochronology model over an empirically calibrated one is the ability to rely on physics to interpolate or extrapolate over parts of parameter space with sparse data coverage. However, rotational spin-down is a complex process that is not yet fully understood and currently no physical model can accurately reproduce all the data available. For this reason, even physically motivated gyrochronology models cannot always be used to reliably extrapolate into unexplored parameter space. Physical models, when calibrated to data can provide insight into the physics of stars however, if accurate and precise *prediction* of stellar properties is desired, empirical models can have advantages over physical ones. For example, the data may reveal complex trends that cannot be reproduced with our current understanding of the physical processes involved but may be captured by more flexible data-driven models. In addition, it is relatively straightforward to build an element of stochasticity into empirical models, *i.e.* to allow for and incorporate outliers or noisy trends. This may be particularly important for stellar spin down, which

does not always seem to behave predictably. A further advantage of empirical models is that inference is more tractable: it can be extremely fast to fit them to data. We use a simple, empirical, deterministic gyrochronology model in this work, which, like any other gyrochronology model, cannot yet reproduce all the observed data. Simple modifications could be made to this model to produce significant improvements, for example, by including instrinsic scatter and outliers, however we leave these improvements for a future project. Ultimately, the model we present here will provide a baseline against which more physically motivated models can be compared.

Despite significant advances in both theoretical and empirical gyrochronology models, no existing model is currently able to reproduce the data. New high quality rotation periods recently measured from Kepler/K2 observations reveal that rotational evolution is more complicated than previously thought, partly because the shape of the rotation-color relation is different and unique for each cluster (Meibom et al. 2011, 2015; Rebull et al. 2016; Douglas et al. 2016; Rebull et al. 2017; Douglas et al. 2017) and partly because stars appear to stop spinning down at old ages (Angus et al. 2015; van Saders et al. 2016, 2018). Theoretical models have been developed to reproduce the lack of magnetic braking at old ages (van Saders et al. 2016, 2018), however no model has yet been designed to fit the individual shape of every cluster. In addition, the relation between rotation period, color and age appears to be stochastic at all ages and masses, particularly for young and low-mass stars. The gyrochronology relations could be improved in three main ways. Firstly, because stellar evolution is a noisy process that produces outliers and scatter, gyrochronology models could be non-deterministic. Secondly, the gyrochronology models could be more flexible in order to capture the inter-cluster variation in the shape of the rotation-color relations. Finally, new calibrators are needed to more precisely constrain rotational evolution at low masses and old ages.

This paper is laid out as follows. In section 2 we describe our new age-dating model and its implementation, in section 3 we test this model on simulated stars, cluster stars and asteroseismic stars, and in section 4 we discuss the implications of these tests and future pathways for development. Throughout this paper we use the word *'observables'* to describe the set of $T_{\rm eff}$, log g, observed bulk metallicity, parallax, photometric color and rotation period observations for a given star. We use the word *'parameters'* to refer to the physical properties of that star: age, mass, true bulk metallicity, distance and V-band extinction that *generate* the observables.

2. Method

A common approach to stellar age-dating is to make separate age predictions using separate sets of observables. For example, if a star's rotation period, parallax, and apparent magnitudes in a range of bandpasses are available, it is possible to predict its age from both gyrochronology and isochrone fitting separately. How these two age predictions are later combined is then a difficult choice. Is it best to average these predictions, to use the more precise of the two, or the one believed to be more accurate? The methodology described here provides an objective method for combining age estimates. There is, after all, only one age for each star. In Bayesian statistics, combining information from different models can be relatively simple, as long as the processes being modeled; those that generated the data, are independent. In this case, we are combining information that relates to the burning of hydrogen in the core (this is the process that drives the slow increase in T_{eff} and luminosity over time) with information about the magnetic braking history of a star (the current rotation period). We can assume that, to first order, these two processes are independent: the hydrogen fraction in the core does not affect a star's rotation period and vice versa. In practise, we can never be entirely sure that two such processes are independent but, at least within the uncertainties, any dependence here is unlikely to affect our results. If this assumption is valid, the likelihoods calculated using each model can be multiplied together.

The desired end product of this method is an estimate of the non-normalized posterior probability density function (PDF) over the age of a star,

$$p(A|\mathbf{m_x}, T_{\mathrm{eff}}, \log g, \hat{F}, P, \bar{\omega}), \tag{1}$$

where A is age, $\mathbf{m_x}$ is a vector of apparent magnitudes in various bandpasses (in our model $\mathbf{m_x} = [m_J, \ m_H, \ m_K]$), $\hat{F}$ is the *observed* bulk metallicity, P is the rotation period and $\bar{\omega}$ is parallax. In order to calculate a posterior PDF over age, we must marginalize over parameters that relate to age, but are not of interest in this study: mass (M), distance (D), V-band extinction (A_V) and the *inferred* bulk metallicity, F. The marginalization involves integrating over these extra parameters,

$$p(A|\mathbf{m_x}, T_{\mathrm{eff}}, \log g, \hat{F}, P, \bar{\omega}) \tag{2}$$
$$\propto \int p(\mathbf{m_x}, T_{\mathrm{eff}}, \log g, \hat{F}, P, \bar{\omega}|A, M, D, A_V, F) \ p(A)p(M)p(D)p(A_V)p(F)dMdDdA_VdF.$$

This equation is a form of Bayes' rule,

$$\mathrm{Posterior} \propto \mathrm{Likelihood} \times \mathrm{Prior}, \tag{3}$$

where the likelihood of the data given the model is,

$$p(\mathbf{m_x}, T_{\mathrm{eff}}, \log g, \hat{F}, P, \bar{\omega}|A, M, D, A_V, F), \tag{4}$$

and the prior PDF over parameters is,

$$p(A)p(M)p(D)p(A_V)p(F). \tag{5}$$

Not all of the observables on the left of the '|' in the likelihood depend on all of the parameters to the right of it. For example, rotation period, P doesn't depend on V-band extinction, A_V. In our model, we make use of conditional independencies like this and use them to factorize the likelihood. Instead of the likelihood we wrote in equation 3, where every observable depends on every parameter, our model can be factorized as,

$$p(\mathbf{m_x}, T_{\text{eff}}, \log g, \hat{F}, \bar{\omega}, C_{B-V}|A, M, D, A_V, F) \; p(P|A, C_{B-V}), \tag{6}$$

where we have introduced a new parameter, C_{B-V}, which is the $B-V$ color that is often used as a mass proxy in the literature. In our model C_{B-V} is not measured but *inferred*: it is a latent parameter. We infer C_{B-V} because all *Kepler* stars have 2MASS photometry in J, H and K bands but do not all have B and V band colors. However, the gyrochronology model we use is calibrated to B-V color, not J-K or otherwise. A probabilistic graphical model (PGM) depicting the joint probability over parameters and observables is shown in figure 3. It describes the conditional dependencies between parameters (in white circles) and observables (in grey circles) with arrows leading from the causal processes to the dependent processes. For example, it is the mass, age, metallicity, extinction and distance that determines the observed spectroscopic properties (T_{eff}, $\log g$ and [Fe/H]) and apparant magnitudes (m_J, m_H and m_K). These parameters also determine the B-V color of a star. In turn, it is a star's age and B-V color that determine its rotation period. Note that, written this way, stellar rotation periods do not directly depend on stellar mass. Mass determines C_{B-V} and C_{B-V}, along with age determines rotation period. The purpose of this PGM is not to depict the physical realities of stellar evolution, it is only a visual description of the structure of the model we use here. Breaking up the problem this way allows us to efficiently join isochronology and gyrochronology and infer the joint age of a star from all its observables. It may well be that rotation period depends directly on mass and metallicity in reality, but it is more practical for us to assume that these dependencies are weak enough not to significantly affect the ages that we ultimately infer.

The factorization of the likelihood described in equation 6 and depicted in figure 3 allows us to multiply two separate likelihood functions together: one computed using an isochronal model and one computed using a gyrochronal model. We assume that the probability of observing the measured observables, given the model parameters is a Gaussian and that the observables are identically and independently distributed. These assumptions allow us to use Gaussian likelihood functions. The isochronal likelihood function is,

$$\mathcal{L}_{\text{iso}} = p(\mathbf{m_x}, T_{\text{eff}}, \log g, \hat{F}, \bar{\omega}, C_{B-V}|A, M, D, A_V, F) \tag{7}$$

Fig. 3.— A probabilistic graphical model (PGM) showing the conditional dependencies between the parameters (white nodes) and observables (gray nodes) in our model. θ is a vector of *parameters*: mass, observed bulk metallicity, distance and V-band extinction; and $\mathbf{O}$ is a vector of *observables*: apparent magnitudes, effective temperature, surface gravity, observed bulk metallicity, and parallax. The observables, $\mathbf{O}$, are determined by the parameters, A and θ. C_{B-V} is a latent parameter that is also determined by the parameters A and θ. In our model, the rotation period observable, P, is determined *only* by the age, A, and color C_{B-V} parameters. The dependencies of observables on parameters and parameters on parameters are indicated by arrows that start at a 'parent' node and end at the dependent observable, or 'child' node. In our model, rotation period does not directly depend on distance, extinction, metallicity or mass, only age and B-V color. This PGM is a representation of the factorized joint PDF over parameters and observables which is written in equation 6.
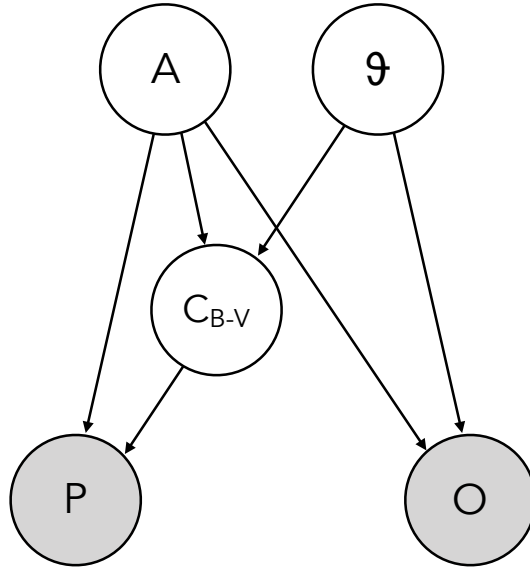
$$= \frac{1}{\sqrt{(2\pi)^n \det(\Sigma)}} \exp\left(-\tfrac{1}{2}(\mathbf{O_I} - \mathbf{I})^T \Sigma^{-1}(\mathbf{O_I} - \mathbf{I})\right),$$

where $\mathbf{O_I}$ is the vector of n observables: T_{eff}, $\log g$, $\hat{F}$, $\bar{\omega}$, m_j, m_h and m_k and Σ is the covariance matrix of that set of observables. $\mathbf{I}$ is the vector of *model* observables that correspond to a set of parameters: A, M, F, D and A_V, calculated using an isochrone model. We assume there is no covariance between these observables and so this covariance matrix consists of individual parameter variances along the diagonal with zeros everywhere else. The gyrochronal likelihood function is,

$$\mathcal{L}_{\text{gyro}} = p(P|A, C_{B-V}) \tag{8}$$
$$= \frac{1}{\sqrt{(2\pi) \det(\Sigma_P)}} \exp\left(-\tfrac{1}{2}(\mathbf{P_O} - \mathbf{P_P})^T \Sigma^{-1}(\mathbf{P_O} - \mathbf{P_P})\right),$$

where $\mathbf{P_O}$ is a 1-D vector of observed rotation periods, $\mathbf{P_P}$ is the vector of corresponding predicted rotation periods, calculated using the vector of inferred ages and C_{B-V} values predicted by the isochronal model. The full likelihood function used in our model is the product of these two likelihood functions,

$$\mathcal{L}_{\text{full}} = \frac{1}{\sqrt{(2\pi)^n \det(\Sigma)}} \exp\left(-\tfrac{1}{2}(\mathbf{O_I} - \mathbf{I})^T \Sigma^{-1}(\mathbf{O_I} - \mathbf{I})\right) \tag{9}$$
$$\times \frac{1}{\sqrt{(2\pi) \det(\Sigma_P)}} \exp\left(-\tfrac{1}{2}(\mathbf{P_O} - \mathbf{P_P})^T \Sigma^{-1}(\mathbf{P_O} - \mathbf{P_P})\right).$$

We place priors over the model parameters A, M, F, D and A_V. These priors represent our 'prior beliefs' about the values these parameters will take, before we use the data to update those beliefs via a likelihood and produce a 'posterior' belief about their values. These priors are described in the appendix.

The gyrochronology model we use to predict P_P is,

$$P = A^\eta \alpha (B - V - \delta)^\beta, \tag{10}$$

where P is rotation period in days, $B - V$ is a star's color, A is stellar age in Myrs and η, α, β and δ take values 0.55, 0.4, 0.31 and 0.45 respectively. This functional form was introduced by (Barnes 2007) and the parameter values are adopted from the recalibration performed in Angus et al. (2015), which is based on young cluster stars and old asteroseismic stars and incorporates a Gaussian mixture model that prevents outliers from influencing the fit. Although this model has been calibrated using a number of cluster stars, it does not provide a good fit to any individual cluster. No current gyrochronology model is able to capture the behavior of rotation as a function of color and age for individual benchmark clusters: the shape of this relation is different in each. The models are not flexible enough to capture inter-cluster differences in rotational evolution. For this reason, we explored the

rotational evolution of a *single* cluster, in order to produce a best-case model and demonstrate the potential of rotation-dating in a case where the model is perfectly accurate. We chose Praesepe as it is a relatively old open cluster (~ 650 Myrs citation), meaning its Solar-type members have converged onto the rotational main sequence, and it is relatively compact on the sky so many of its members were observed during a single *K2* campaign. In fact, Praesepe was repeatedly observed by *K2*, in Campaigns 5, 16 and 18, however we only use rotation periods published from the analysis of Campaign 5 in this work.

We used a three-dimensional polynomial model to predict rotation period as a function of *Gaia* color and age for Praesepe and the Sun. This model consists of a 4th order polynomial in logarithmic Gaia color: $G_{Bp} - G_{Rp}$, which we write as C_G for simplicity, and a 1st order polynomial (a straight line) in logarithmic age. We switched to using $G_{Bp} - G_{Rp}$ because, due to the $\sim$ billion stars observed by *Gaia*, it is now the most abundant and widely available photometric color. Our gyrochronology likelihood function is designed to compare observed rotation period to predicted rotation period. For this reason the gyrochronology model we used must predict rotation period as a function of age and color. However, when *calibrating* the gyrochronology model, we chose to make *age* the dependent variable because the uncertainties on age are much greater than the uncertainties on rotation period. Since we are using a linear model, the relation is easily invertable. We fitted the following model to Praesepe members:

$$\log_{10}(A) = a + b \log_{10}(C_G) + c \log_{10}^2(C_G) + d \log_{10}^3(C_G) + e \log_{10}^4(C_G) + f \log_{10}(P) \quad (11)$$

where P is rotation period in days, C_G is Gaia color, A is stellar age in years and the lower case letters are free parameters which we fitted to the data using linear least squares. We adopted an age for Praesepe of 650 million years citation, a Solar age of 4.56 Gyr citation, and a Solar rotation period of 26 days citation. The Sun's color in the Gaia color bandpasses, $G_{Bp} - G_{Rp}$, is 0.82 (Casagrande and VandenBerg 2018). We found best-fit values: $a = 7.37 \pm 0.03, b = -1.4 \pm 0.1, c = 5.0 \pm 0.8, d = -34 \pm 3, e = 66 \pm 14$, and $f = 1.49 \pm 0.02$. Rotation periods for Prasepe were obtained from **?** and their *Gaia* colors were obtained by crossmatching their sky-projected positions with the *Gaia* DR2 catalog. We inverted this relation to predict rotation period as a function of color and age,

$$\log_{10}(P) = \frac{\log_{10}(A) - a - b \log_{10}(C_G) - c \log_{10}^2(C_G) - d \log_{10}^3(C_G) - e \log_{10}^4(C_G)}{f}. \quad (12)$$

We used both equations **??** and 12 to predict the ages of individual Praesepe stars from their rotation periods and apparent magnitudes in section 3.

It was recently shown that a simple power law in age does not provide a good fit to old asteroseismic stars (Angus et al. 2015; van Saders et al. 2016). It is hypothesized that the

magnetic braking of these old stars has ceased and cannot be modeled with a Skumanich-like spin-down law (van Saders et al. 2016). In future, the above model could and should be updated to include a more flexible treatment of rotation period as a function of age in order to account for the change of slope in the relation. Until then, this method should only be used for stars with Rossby number below 2.1 (van Saders et al. 2016), *i.e.* their ratio of rotation period to convection overturn time ($P/\tau = Ro$) does not exceed 2.1. In this work we are chiefly concerned with introducing a new framework where rotation periods are modeled *simultaneously* with isochronal features. Although this gyrochronology model does not provide a good fit to all the available data, we reiterate that no single model *is* able to reproduce all the data, and that there is utility in using such a simple, linear, empirical model like this. Again, we are not attempting to improve gyrochronology models in this work: in this paper we are more concerned with introducing a new approach to modeling stellar ages, however, our method is highly flexible and modular and an improved gyrochronology model could easily be swapped in for this one in future. Our model allows a linear combination of other, *physical* parameters to be used to predict age from rotation period, like $\log g$, metallicity and mass. In future, it may be better to model stars in physical rather than observable parameter space.

To calculate **I**, the vector of predicted isochronal observables, we use the `isochrones.py` *python* package which has a range of functionalities relating to isochrone fitting. The first of the `isochrones.py` functions we use is the likelihood function of equation 8. The `isochrones.py` likelihood function accepts a dictionary of observables which can, but does not *have* to include, all of the following: $T_{\rm eff}$, $\log g$, [Fe/H], parallax and apparent magnitudes in a range of colors, as well as the uncertainties on all these observables. It then calculates the residual vector $(\mathbf{O_I} - \mathbf{I})$ where $\mathbf{O_I}$ is the vector of observables and **I** is a vector of corresponding predicted observables. The prediction is calculated using a set of isochrones (we use the MIST models **?**), where the set of *model* observables that correspond to a set of physical parameters is returned. This requires interpolation over the model grids since, especially at high dimensions, it is unlikely that any set of physical parameters will exactly match a precomputed set of isochrones. The observables that correspond to a set of physical parameters (age, mass, etc) go into **I** and the `isochrones.py` likelihood function returns the result of equation 8. The second `isochrones.py` function we use is one that querys the best-fit isochrone model chosen to predict **I**, in order to predict the corresponding C_{B-V} for that star. This color is then used to calculate the gyrochronal likelihood function of equation 9.

The inference processes procedes as follows (as a reminder, we use *observables* to refer to the data: $T_{\rm eff}$, $\log g$, etc and *parameters* to refer to the model parameters: age, mass, etc). First, a set of parameters: age, mass, true bulk metallicity, distance and extinction, as

well as observed values of $T_{\rm eff}$, log g, bulk metallicity, 2MASS colors and parallax ($\mathbf{O_I}$) for a single star are passed to the isochronal likelihood function (equation 8). Then, a set of *model* values of $T_{\rm eff}$, log g, bulk metallicity, 2MASS colors and parallax ($\mathbf{I}$) that correspond to that set of parameters are calculated by `isochrones.py`. The isochronal log-likelihood, $\ln(\mathcal{L}_{\rm iso})$, is then computed for these parameter values. The same age that was passed to the likelihood function, and the C_{B-V} corresponding to it, along with the observed rotation period, are then passed to the gyrochronal likelihood function (equation 9). The gyrochronal log-likelihood, $\ln(\mathcal{L}_{\rm gyro})$, is computed. The full log-likelihood is then calculated,

$$\ln(\mathcal{L}_{\rm full}) = \ln(\mathcal{L}_{\rm iso}) + \ln(\mathcal{L}_{\rm gyro}), \tag{13}$$

and added to the log-prior to produce a single sample from the posterior PDF.

We sampled the joint posterior PDF over age, mass, metallicity, distance and extinction using the affine invariant ensemble sampler, `emcee` (**?**). We used 24 walkers and sampled the posterior PDF until 100 *independent* samples were obtained. We estimated the autocorrelation length, indicating how many steps are taken per independent sample, after every 100 steps using the autocorrelation tool built into `emcee`. We stopped obtaining samples when either *both* 100 times the autocorrelation length was reached *and* the change in autocorrelation length over 100 samples was less than 0.01, or the maximum of 100,000 samples was obtained. This allowed use to continue obtaining samples from the posterior This provided an average of ... non-independent samples. The method described above is trivially parallelizable, since the inference proccess for each star can be inferred on a separate node. Running our code on a cluster, we found that a posterior PDF can be estimated for a single star in around one minute.

3. Results

In order to demonstrate the functionality of our method, we conducted two tests. In the first we simulated a set of observables from a set of fundamental parameters for a few hundred stars using the MIST (**?**) stellar evolution models. In the second we tested our model by attempting the measure the ages of stars in the Praesepe open cluster who's age has been measured precisely because it is an ensemble of coeval stars with the same metallicity; a single stellar poplulation, and its age can be established through isochrone fitting and MS turn-off.

For the first test we began with a set of 1000 stars and drew masses, ages, bulk metallicities, distances and extinctions at random from the following uniform distributions:

$$M \sim U(0.5, 1.5) \ [M_\odot] \tag{14}$$
$$A \sim U(0.5, 14) \ [\text{Gyr}] \tag{15}$$
$$F \sim U(-0.2, 0.2) \tag{16}$$
$$D \sim U(10, 1000) \ [\text{pc}] \tag{17}$$
$$A_V \sim U(0, 1). \tag{18}$$

T_{eff}, $\log g$, $\hat{F}$, m_x, $\bar{\omega}$ and B-V were then generated using these stellar parameters with the MIST stellar evolution models (**?**) and rotation periods, P were generated from the gyrochronology relation in equation 10 with age, A, and B-V. We then performed cuts on these simulated stars to remove evolved stars and stars that are too hot. The rotation periods of evolved stars, defined here to be those with $\log g$ ¿ 4.5 begin to increase as soon as they turn off the MS and their radii start to enlarge and cannot be modeled with the gyrochronology relation of equation **??**. In addition, hot stars (defined as 6250 K ¡ T_{eff}) cannot be modeled using equation **??** because their convective envelopes are extremely shallow and their magnetic fields are weaker, leading to a lack of magnetic braking. The rotation periods of these stars do not increase substantially during their time on the MS. After performing these cuts, 649 update stars remained in the sample of simulated stars. We took two approaches to inferred the ages of these simulated stars: firstly using *only* a stellar evolution model, and secondly using a stellar evolution model *combined with* a gyrochronology model. For all stars, our initial guesses for the parameters are $M = 1M_\odot$, $A = 1$ Gyr, $F = 0$, $D = 500$ pc and $A_V = 0.1$.

Figure 4 shows the results of using a stellar evolution model model to estimate the posterior PDFs over the stellar ages of simulated stars. The rotation periods of stars have not been incorporated into this model: these posterior PDFs were obtained by isochrone fitting only, using the likelihood function in equation 8. In most cases ages are only weakly

Fig. 4.— The results of a test in which we simulated observable properties of stars with the same model we used to infer their properties. In this experiment we used *only* stellar evolution models to infer ages; we did not use rotation periods. For results where we used *both* stellar evolution models *and* gyrochronology, see figure 5. The true age, used to produce associated observables is shown on the x-axis, and the ages we inferred are shown on the y-axos. This figure shows the posterior PDFs over stellar age for each of the simulated stars as a 'violin plot', where samples from the posterior are plotted vertically as a smooth, symmetric function. The widths of these functions indicates the probability over age: wider regions represent more probable ages. The median values of the posterior PDFs are plotted as solid horizontal lines. This figure demonstrates that when only stellar evolution models are used to infer ages for field MS stars, the resulting predicted ages are extremely imprecise.
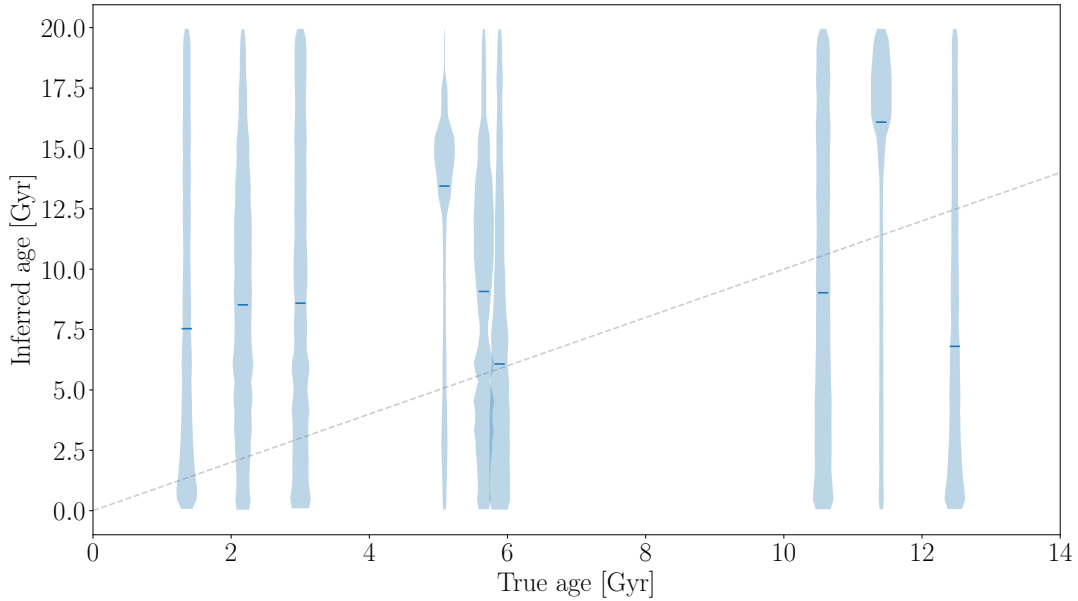
Fig. 5.— The results of a test in which we simulated observable properties of stars with the same model we used to infer their properties. In this experiment we used *both* stellar evolution models to rotation periods to infer ages. For results where we used stellar evolution models *only*, see the previous figure (figure 4). The true age, used to produce associated observables is shown on the x-axis, and the ages we inferred are shown on the y-axis. This figure shows the posterior PDFs over stellar age for each of the simulated stars as a 'violin plot', where samples from the posterior are plotted vertically as a smooth, symmetric function. The widths of these functions indicates the probability over age: wider regions represent more probable ages. The median values of the posterior PDFs are plotted as solid horizontal lines. This figure demonstrates that when rotation periods (gyrochronoloy) *and* stellar evolution models are used to infer the ages of field MS stars, the resulting predicted ages relatively precise; much more precise than when using stellar evolution models alone.
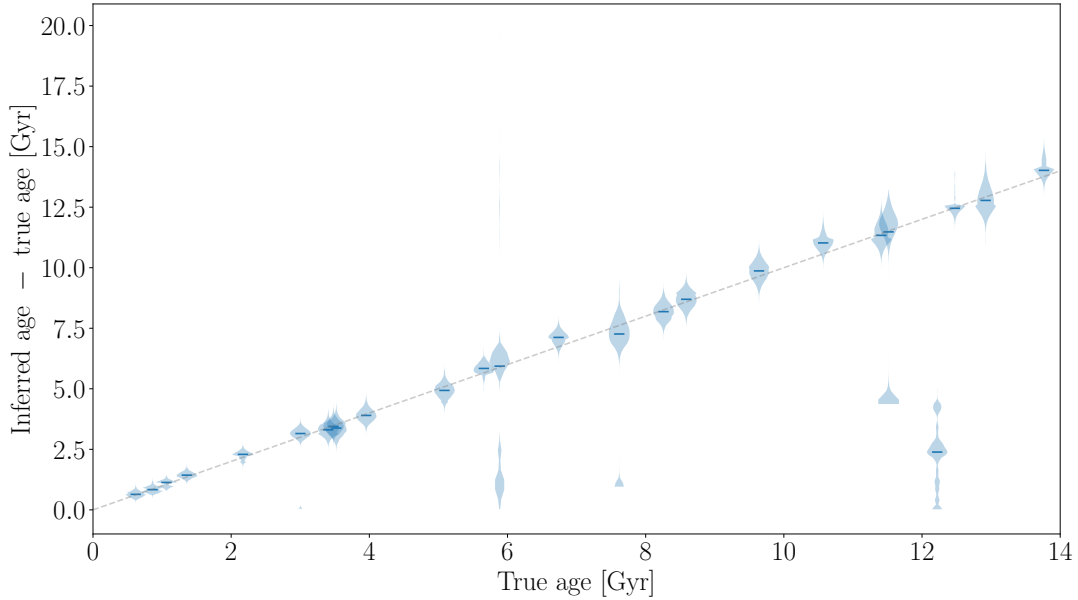
constrained by the stellar evolution models. In some cases there is no constraint on the stellar age: the age of the star is consistent with all ages from 0-14 Gyrs. The reason for this is that the temperatures and luminosities of stars do not change very much on the main sequence. The isochrones are tightly spaced in the MS region of the HR-diagram and, as a result, even precisely measured temperatures and luminosities often do not yield precise ages. Figure 5 shows the results of using a stellar evolution, combined with a gyrochronology model. These ages have been inferred using the likelihood of equation 13. Again, the true stellar ages are plotted on the x-axis and the posterior PDFs of the inferred ages are plotted on the y-axis. Here, unlike the case where only stellar evolution models were used, the recovered ages are precise. This is because gyrochronology isochrones (or gyrochrones) are more widely separated relative to the observational uncertainties than the isochrones used above. Put another way, the rotation periods of two stars of different ages and the same mass will have rotation periods that differ significantly – almost certainly more than the observational uncertainty on rotation period. On the other hand, two stars of the same mass and different age are likely to have extremely similar luminosities and temperatures and the differences between these properties are likely to be smaller than the observational uncertainties.

Figure **??** demonstrates the results of inferring ages using rotation periods only, and this illustrates why the combination of isochronal and gyrochronal ages is so precise: almost all this precision comes from rotation periods. This simulation experiment is unrealistic for two main reasons: firstly, we simulated data from the same gyrochronology model we used to infer ages and so the results will be perfectly accurate by design. Secondly, we simulated data without any intrinsic scatter built into the gyrochronology model; it is a deterministic model. This means that a rotation period and color predicts a corresponding single-valued age, rather than a probability distribution over ages. This is unrealistic given observations of open clusters who's members clearly show excess scatter in their rotation periods, particularly for less massive stars. These results look precise and accurate, but this is misleading. Inaccuracies would arise if the gyrochronology model was incorrect or poorly calibrated in all parts of parameter space and imprecision would arise if intrinsic scatter were built into the gyrochronology model. The result of using a deterministic model, such as the one used in this experiment, is that the uncertainties on stellar ages will be unrealistically small.

In this experiment, we compared the precision of MS field star ages inferred with stellar evolution models only, and with stellar evolution models *combined* with gyrochronology models. We showed that including gyrochronology in the stellar evolution model results in much more precise age predictions. We have not yet made any statement about accuracy however; the above experiment produces accurate ages by construction. In order to test the

potential of this method to produce accurate results, we test our model on real data in the following section.

In order to test our model on real stars with known ages, we selected a sample of cluster stars with precisely measured ages from ensemble isochrone fitting and main sequence turn off. The ages of open clusters can be measured much more precisely than field stars for two main reasons. Firstly, the stars have the same age (to within a few million years), so the age of a cluster can be inferred with an increased precision that is proportional to the square root of the number stars, relative to a single star case. In addition, stars in the same cluster form (we assume) from the same molecular cloud and therefore have the same metallicity. Since cluster stars have the same metallicity and age, stars fall on the same isochrone and the main sequence turn off can be identified. We compiled rotation periods and Gaia photometry and parallaxes for members of Praesepe, a 650 Myr cluster. We chose Praesepe because it is relatively tightly clustered on the sky and many of its members were therefore targeted in a single *K2* campaign, from which it was possible to measure rotation periods via frequency analysis of member's light curves (**?**). We crossmatched N Praesepe members with measured rotation periods (**?**), with the Gaia DR2 catalog Gaia DR2 citation, using a 5" search radius. The result was a sample of N stars with rotation periods, parallaxes and *Gaia G*, G_{BP} and G_{RP} -band photometry. Figure **??** shows the rotation periods of Praesepe members as a function of their dust-corrected *Gaia* $G_{Bp} - G_{Rp}$ colors. We used the `dustmaps python` package to calculate dust extinction along the line of sight to these stars. The filled blue circles show the FGK stars on the 'rotational main sequence' that were used to calibrate a relation between rotation period and color for this cluster.

In order to fit a period-color relation to these data we restricted the sample of cluster stars to the color range, $0.56 < G_{Bp} - G_{Rp} < 3$ in order to remove early F and late M dwarfs whos' rotation periods do not fall on the 'gyrochronology main sequence'. Although it *may* be possible to crudely predict the ages of these stars (at least the M dwarfs) from their rotation periods, the age-rotation-color relation for these stars is very different to the FGK star relations and is not the focus of this paper. In addition, we removed rapidly rotating stars from the sample since, although modeling outliers is important and consequential for gyrochronology in general, the goal of this paper is not to produce a perfect gyrochronology that reproduces stochasticity in the data, just a simple function that fits the rotational main sequence of Praesepe. In future we plan to update the gyrochronology models to include M dwarfs, and the outlying rapid rotators using a mixture of Gaussians. Similarly, we used only Praesepe in this study because the period-color relations of each open cluster with rotation periods has a different shape. This is likely due to differences in metalicities, incomplete or noisy membership lists and differences in rotation period measurement algorithms. A global gyrochronology calibration, using all cluster data is planned for the future but, again,

is beyond the scope of the project presented here. The rotation periods of the Praesepe members in the restricted color range and with outliers removed are plotted against their *Gaia* colors in figure **??**. We used linear least squares to fit a linear model to Praesepe and the Sun. A 4th order polynomial in $\log(G_{BP} - G_{RP})$ and a straight line in $\log(\text{Age [yrs]})$ was fit to reproduce $\log(\text{rotation period [days]})$.

$$\log(P) = a + b\log(C_G) + c\log^2(C_G) + d\log^3(C_G) + e\log^4(C_G) + f\log(A), \qquad (19)$$

were P is period, C_G is $Gaia\, G_{Bp} - G_{Rp}$ color, and A is age.

The resulting ages predicted for individual members of Praesepe (where each member is treated as an isolated field star) are shown in figure **??**. Figure **??** demonstrates the power of incorporating gyrochronology into stellar evolution models. The orange distributions show individual posterior PDFs over stellar age for each member of Praesepe, where ages were inferred using stellar evolution models *only*, with *Gaia* colors ($G_{Bp} - G_{Rp}$), *Gaia* apparent magnitude (G), and *Gaia* parallaxes as the observable properties. The blue distributions are posterior PDFs over stellar age for each member of Praesepe, where ages were inferred using stellar evolution models *and* a gyrochronology model. The blue posteriors are much more strongly peaked around the true age of the cluster and this demonstrates that rotation periods carry far more age information than photometric colors, even when parallaxes are available. The median age of Praesepe members, as predicted using stellar evolution models only is .... and the median standard deviation of the age measurements (the median spread in the orange posteriors of figure **??**) is .... In contrast, the median age of Praesepe members, as predicted using stellar evolution models *and* gyrochronology (the blue posteriors in figure **??**) is ... and the median standard deviation of these posteriors is....

Stellar rotation periods are age-informative and so including them in our analysis leads to the more precise measurement of ages. However, rotation periods do not carry very much information about the metallicity of a star, nor their distance. They are also not particularly informative about the mass of a star because rotation periods depend on both mass and age, and stellar mass is strongly informed by color and temperature information, so the mass of a star is determined from the stellar evolution models. However, age, mass and metallicity are correlated: a star can be more blue because it is more massive, older or more metal poor. For this reason, if a star's age is more tightly constrained, constraints on mass and metallicity will also improve. Figures ... and ... show the differences in posterior PDFs over metallicity and mass respectively, calculated for Prasepe stars where rotation period information is both used (blue posteriors) and not used (orange posteriors). The black line in figure ... shows the metallicity of Prasepe citation. There is little difference between blue and orange because rotation periods do not strongly depend on metallicity or mass (independantly of age). However, the precision of mass and metallicity measurements is slightly improved due

Fig. 6.— The rotation periods of Praesepe members and the Sun, plotted against their *Gaia* colors ($G_{Bp} - G_{Rp}$) in logarithmic space. We fit a linear model to these data in order to predict rotation periods from *Gaia* colors and age. This model consisted of a fourth-order polynomial in $\log_{10}$ color, and a 1st order polynomial (a straight line) in $\log_{10}$ age. The result of this fit is plotted on top of the data at the ages of Praesepe and the Sun.
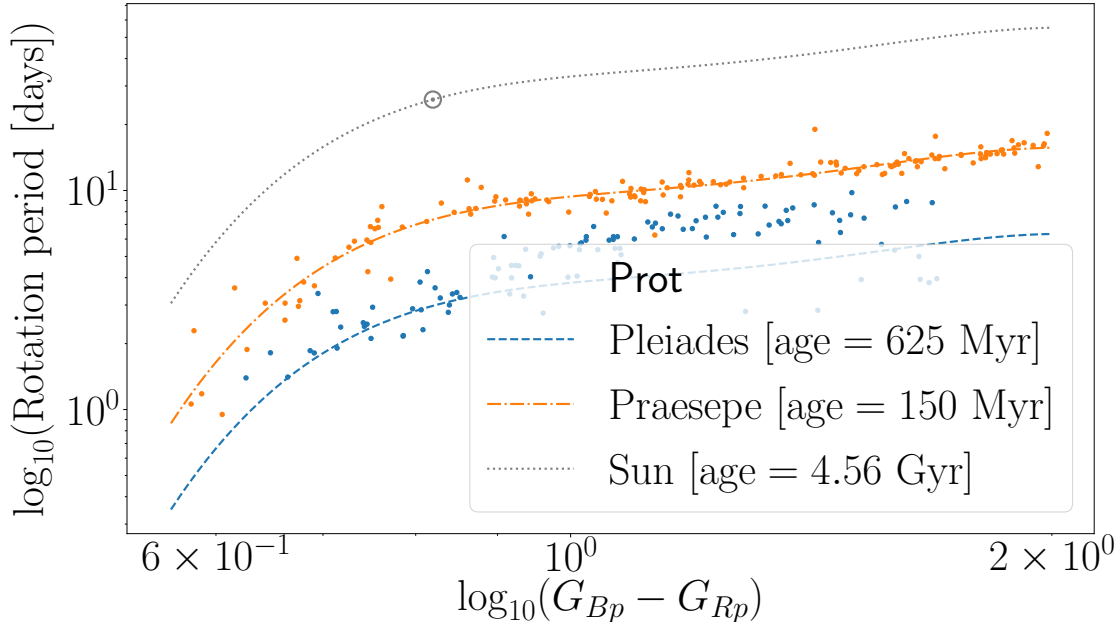
to the fact that age, mass and metallicity are correlated. In this example of fitting our model to Prasepe data, we use *Gaia* parallaxes which are extremely informative about the distances to stars and increasing the information about stellar ages is unlikely to propoagate through to these distances at a meaningful level.

The results in figure **??** were produced using a gyrochronology relation (equation **??**) that was calibrated using the Hyades, Coma Berenices and Pleiades clusters, plus the Sun and old asteroseismic stars (Angus et al. 2015). Figure **??** however, shows the results of inferring the ages of Praesepe members with the dedicated Praesepe gyrochronology relation of equation 12. We include these results because we would like to provide an idea of the kind of age measurement accuracy that is achievable in the best case: where the gyrochronology model perfectly reproduces the data.

To summarize the results of this section of the paper: fitting our new age model to simulated stars and members of the Praesepe cluster (an open cluster with a precisely measured age from ensemble isochrone fitting and MS turn-off) demonstrates that using stellar evolution models *alone* to calculate the ages of cool MS dwarf stars results in extremely imprecise ages, however when gyrochonology is incorporated, the precision of age measurements increase significantly.

4. Discussion

In the previous section we demonstrated that modeling the ages of stars using isochrones *and* gyrochronology can result in more precise and accurate ages than using either isochrone fitting or gyrochronology alone.

Isochrone fitting and gyrochronology are extremely complementary because gyrochronology is more precise where isochrone fitting is less precise and vice versa. Age precision is determined by the spacing of isochrones or gyrochrones: in regions where iso/gyrochrones are more tightly spaced, ages will be less precise. Isochrones get less tightly spaced (and more precise) at larger stellar masses and gyrochrones get more tightly spaced (and less precise) at larger stellar masses. Figure **??** shows our simulated star sample on an H-R diagram. Points are positioned by their true properties, not their inferred ones, and colored by their age *precision* as calculated using isochrones and gyrochronology. Paler stars have less precise inferred ages.

The method we present here will be useful for a large number of stars: tens-of-thousands *Kepler* stars already and many more from *TESS, LSST, WFIRST, PLATO, Gaia, PanSTARRS* and more. However, there are also several types of star for which gyrochronology is, in general, *not* useful. This list includes: stars with thin convective envelopes, more massive than around 1 $M_\odot$; fully convectives stars, less massive than around 0.3 $M_\odot$; evolved stars with log g less than around 4.5; stars that haven't converged onto the rotational main sequence, *i.e.* those younger than around 500 Myrs; stars who have ceased magnetic braking, *i.e.* those with Ro greater than around 2.1; synchronised binaries who's rotation periods are locked to their orbital periods; and other classes of gyrochronal outliers. Since many stars with measurable rotation periods do not have precise spectroscopic properties, it is not always possible to tell whether a star falls within these permissable ranges of masses, surface gravities and rossby numbers. In addition, any given star, even if it does meet the criteria for mass, evolutionary stage, age, binarity, etc, may still be a rotational outlier. Rotational outliers are often seen in clusters (see *e.g.* **?**). In any case where a star's age is not truly represented by its rotation period, its isochronal age will be in tension with its gyrochronal one. However, given the precision of the gyrochronal technique, the gyrochronal age may dominate over the isochronal one. Figure **??** shows the posterior PDF for a star with a misrepresentative rotation period. This star is rotating more rapidly than its age and mass indicate it should, so the gyrochronal age of this star is under-predicted. Situations like this are likely to arise relatively often, partly because rotational spin-down is not a perfect process and some unknown physical processes can produce outliers, and partly because misclassified giants, hot stars, M dwarfs or very young or very old stars will not have rotation periods that relate to their ages in the same way. In addition, measured rotation periods may not always be

accurate and in many cases, due to aliasing, can be a harmonic of the true rotation period. One of the more common rotation period measurement failure modes is to measure half the true rotation period. The best way to prevent an erroneous or outlying rotation period from resulting in an erroneous age measurement is to *allow* for outlying rotation periods using a mixture model.

Throughout this manuscript we have referred to the 'accuracy' of the isochronal models. In reality though, stellar evolution models are not 100% accurate and different stellar evolution models, *e.g.*, MIST, Dartmouth, Yonsei-Yale, etc will predict slightly different ages. The disagreement between these models varies with position on the HR diagram, but in general, ages predicted using different stellar evolution models will vary by around 10%. We use the MIST models in our code because they cover a broader range of ages, masses and metallicities than the Dartmouth models.

Our focus so far has been on stellar age because this is the most difficult stellar parameter to measure. However, if the age precision is improved, then the mass, [Fe/H], distance and extinction precision must also be improved, since these parameters are strongly correlated and co-dependent in the isochronal model. Figure **??** shows the improvement in relative precision of mass measurements from our simulated star sample.

5. Conclusion

We have presented a statistical framework for joining together observations of different stellar properties that relate, via different evolutionary processes, to stellar age. Specifically, we combine information used to place stars on an isochrone in an HR diagram: T_{eff}, log g, observed bulk metallicity, parallax and photometric colors with rotation periods, used to date stars via their magnetic braking history. The two methods of ischrone fitting and gyrochronology are simply combined by taking the product of two likelihood functions: one that contains an isochronal model and the other a gyrochronal one. The isochronal model is based on the MIST stellar evolution model (**?**) and computed using `isochrones.py`. The gyrochronal model is a simple 2-dimensional power-law relation between rotation period, B-V color and age. It is based on the functional form first introduced by Barnes (2003) and later recalibrated by Angus et al. (2015).

We tested this age-dating model on simulated data, cluster stars and asteroseismic stars with precisely measured ages. The age of the Hyades is generally measured using stellar evolution/isochrone models where the ensemble of stars at the same age but a *range of masses* allows a very precise isochronal age to be inferred. In particular, this allows the main sequence-turn off to be identified which, since it appears as a sharp feature in a mono-age population, allows the age of the population to be precisely inferred. We found that this model predicts ages that are an order of magnitude more precise than using isochrone fitting alone. However, we caution users of this method that our choice of gyrochronology model is not suitable for stars outside a specific range of stellar parameters, described in the text.

In the future we hope to make several improvements to the gyrochronology relation used here, including, allowing for outliers via a mixture model, including intrinsic scatter and/or replacing the power-law with a semi-parametric model.

The code used in this project is available as a documented *python* package called `chronology`. It is available for download on Github or through Pypi (pip install chronology). The documentation is available at readthedocs..... The exact version used to produce the results here is available under add github hash.

6. Appendix

Priors

We use the default priors in the `isochrones.py` *python* package. The prior over age is,

$$p(A) = \frac{\log(10)10^A}{10^{10.5} - 10^8}, \quad 8 < A < 10.5. \tag{20}$$

where A, is $\log_{10}(\text{Age [yrs]})$. The prior over mass is uniform in natural-log between -20 and 20,

$$p(M) = U(-20, 20) \tag{21}$$

where M is $\ln(\text{Mass } [M_\odot])$. The prior over true bulk metallicity is based on the galactic metallicity distribution, as inferred using data from the Sloan Digital Sky Survey citation. It is the product of a Gaussian that describes the metallicity distribution over halo stars and two Gaussians that describe the metallicity distribution in the thin and thick disks:

$$p(F) = H_F \frac{1}{\sqrt{2\pi\sigma_{\text{halo}}^2}} \exp\left(-\frac{(F - \mu_{\text{halo}})^2}{2\sigma_{\text{halo}}}\right) \tag{22}$$
$$\times (1 - H_F)\frac{1}{\xi}\left[\frac{0.8}{0.15}\exp\left(-\frac{(F - 0.016)^2}{2\times 0.15^2}\right) + \frac{0.2}{0.22}\exp\left(-\frac{(F - 0.15)^2}{2\times 0.22^2}\right)\right],$$

where $H_F = 0.001$ is the halo fraction, μ_{halo} and σ_{halo} are the mean and standard deviation of a Gaussian that describes a probability distribution over metallicity in the halo, and take values -1.5 and 0.4 respectively. The two Gaussians inside the square brackets describe probability distributions over metallicity in the thin and thick disks. The values of the means and standard deviations in these Gaussians are from **?**. ξ is the integral of everything in the square brackets from $-\infty$ to ∞ and takes the value ~ 2.507. The prior over distance is,

$$p(D) = \frac{3}{3000^3}D^2, \quad 0 < D < 3000, \tag{23}$$

where D is in kiloparsecs. Finally, the prior over extinction is uniform between zero and one,

$$p(A_V) = U(0, 1). \tag{24}$$

REFERENCES

R. Angus, S. Aigrain, D. Foreman-Mackey, and A. McQuillan. Calibrating gyrochronology using Kepler asteroseismic targets. *MNRAS*, 450:1787–1798, June 2015. doi: 10.1093/mnras/stv423.

S. A. Barnes. On the Rotational Evolution of Solar- and Late-Type Stars, Its Magnetic Origins, and the Possibility of Stellar Gyrochronology. *ApJ*, 586:464–479, March 2003. doi: 10.1086/367639.

S. A. Barnes. Ages for Illustrative Field Stars Using Gyrochronology: Viability, Limitations, and Errors. *ApJ*, 669:1167–1189, November 2007. doi: 10.1086/519295.

L. Casagrande and D. A. VandenBerg. On the use of Gaia magnitudes and new tables of bolometric corrections. *MNRAS*, 479:L102–L107, September 2018. doi: 10.1093/mnrasl/sly104.

W. J. Chaplin, S. Basu, D. Huber, et al. Asteroseismic Fundamental Properties of Solar-type Stars Observed by the NASA Kepler Mission. *ApJS*, 210:1, January 2014. doi: 10.1088/0067-0049/210/1/1.

P. Das and J. L. Sanders. MADE: A spectroscopic Mass, Age, and Distance Estimator for red giant stars with Bayesian machine learning. *MNRAS*, October 2018. doi: 10.1093/mnras/sty2776.

S. T. Douglas, M. A. Agüeros, K. R. Covey, P. A. Cargile, T. Barclay, A. Cody, S. B. Howell, and T. Kopytova. K2 Rotation Periods for Low-mass Hyads and the Implications for Gyrochronology. *ApJ*, 822:47, May 2016. doi: 10.3847/0004-637X/822/1/47.

S. T. Douglas, M. A. Agüeros, K. R. Covey, and A. Kraus. Poking the Beehive from Space: K2 Rotation Periods for Praesepe. *ApJ*, 842:83, June 2017. doi: 10.3847/1538-4357/aa6e52.

C. R. Epstein and M. H. Pinsonneault. How Good a Clock is Rotation? The Stellar Rotation-Mass-Age Relationship for Old Field Stars. *ApJ*, 780:159, January 2014. doi: 10.1088/0004-637X/780/2/159.

S. D. Kawaler. Angular momentum loss in low-mass stars. *ApJ*, 333:236–247, October 1988. doi: 10.1086/166740.

S. D. Kawaler. Rotational dating of middle-aged stars. *ApJ*, 343:L65–L68, August 1989. doi: 10.1086/185512.

E. E. Mamajek and L. A. Hillenbrand. Improved Age Estimation for Solar-Type Dwarfs Using Activity-Rotation Diagnostics. *ApJ*, 687:1264–1293, November 2008. doi: 10.1086/591785.

S. P. Matt, A. S. Brun, I. Baraffe, J. Bouvier, and G. Chabrier. The Mass-dependence of Angular Momentum Evolution in Sun-like Stars. *ApJ*, 799:L23, January 2015. doi: 10.1088/2041-8205/799/2/L23.

S. Meibom, S. A. Barnes, D. W. Latham, N. Batalha, W. J. Borucki, D. G. Koch, G. Basri, L. M. Walkowicz, K. A. Janes, J. Jenkins, J. Van Cleve, M. R. Haas, S. T. Bryson, A. K. Dupree, G. Furesz, A. H. Szentgyorgyi, L. A. Buchhave, B. D. Clarke, J. D. Twicken, and E. V. Quintana. The Kepler Cluster Study: Stellar Rotation in NGC 6811. *ApJ*, 733:L9, May 2011. doi: 10.1088/2041-8205/733/1/L9.

S. Meibom, S. A. Barnes, I. Platais, R. L. Gilliland, D. W. Latham, and R. D. Mathieu. A spin-down clock for cool stars from observations of a 2.5-billion-year-old cluster. *Nature*, 517:589–591, January 2015. doi: 10.1038/nature14118.

M. Ness, D. W. Hogg, H.-W. Rix, A. Y. Q. Ho, and G. Zasowski. The Cannon: A data-driven approach to Stellar Label Determination. *ApJ*, 808:16, July 2015. doi: 10.1088/0004-637X/808/1/16.

L. M. Rebull, J. R. Stauffer, J. Bouvier, A. M. Cody, L. A. Hillenbrand, D. R. Soderblom, J. Valenti, D. Barrado, H. Bouy, D. Ciardi, M. Pinsonneault, K. Stassun, G. Micela, S. Aigrain, F. Vrba, G. Somers, J. Christiansen, E. Gillen, and A. Collier Cameron. Rotation in the Pleiades with K2. I. Data and First Results. *AJ*, 152:113, November 2016. doi: 10.3847/0004-6256/152/5/113.

L. M. Rebull, J. R. Stauffer, L. A. Hillenbrand, A. M. Cody, J. Bouvier, D. R. Soderblom, M. Pinsonneault, and L. Hebb. Rotation of Late-type Stars in Praesepe with K2. *ApJ*, 839:92, April 2017. doi: 10.3847/1538-4357/aa6aa4.

J. L. Sanders and P. Das. Isochrone ages for 3 million stars with the second Gaia data release. *MNRAS*, 481:4093–4110, December 2018. doi: 10.1093/mnras/sty2490.

A. Skumanich. Time Scales for CA II Emission Decay, Rotational Braking, and Lithium Depletion. *ApJ*, 171:565, February 1972. doi: 10.1086/151310.

D. Stello, J. Zinn, Y. Elsworth, R. A. Garcia, T. Kallinger, S. Mathur, B. Mosser, S. Sharma, W. J. Chaplin, G. Davies, D. Huber, C. D. Jones, A. Miglio, and V. Silva Aguirre. The K2 Galactic Archaeology Program Data Release. I. Asteroseismic Results from Campaign 1. *ApJ*, 835:83, January 2017. doi: 10.3847/1538-4357/835/1/83.

J. L. van Saders and M. H. Pinsonneault. Fast Star, Slow Star; Old Star, Young Star: Subgiant Rotation as a Population and Stellar Physics Diagnostic. *ApJ*, 776:67, October 2013. doi: 10.1088/0004-637X/776/2/67.

J. L. van Saders, T. Ceillier, T. S. Metcalfe, V. Silva Aguirre, M. H. Pinsonneault, R. A. García, S. Mathur, and G. R. Davies. Weakened magnetic braking as the origin of anomalously rapid rotation in old field stars. *Nature*, 529:181–184, January 2016. doi: 10.1038/nature16168.

J. L. van Saders, M. H. Pinsonneault, and M. Barbieri. Forward Modeling of the Kepler Stellar Rotation Period Distribution: Interpreting Periods from Mixed and Biased Stellar Populations. *ArXiv e-prints*, March 2018.